Yali HOU, Sheng WANG, Zhenlu HAN

School of Mechanical Engineering, Qingdao Technological University, 266033, China

The dynamics modeling and simulation for coupled double-rotor spindle system of high speed grinder

Abstract. *This study was focused on the theoretical modeling and numerical simulation about the dynamic characteristics of coupled double-rotor spindle system of high speed grinder. The critical speeds of first three orders, the modes of variation and other dynamic characteristic parameters of the spindle system were analyzed and calculated. The results showed that the critical speeds of coupled double-rotor system were arranged in a similar increasing order as to those of each single rotor. It was thus indicated that the critical speeds of each order for coupled double-rotor system corresponded to those of single rotor. Furthermore, the main vibration modes of double-rotor system at each order were analyzed. The results indicated that vibration mode of each order of double rotors was the superimposition of the vibration mode of each single rotor. At variable critical speeds, the vibration mode of each single rotor in the system varied in its extent. If the critical speed of double-rotor system was close to that of a single rotor, then the superimposition of vibration modes of single rotors would become more significant under coupling state.*

Streszczenie: *W pracy położono nacisk na modelowanie teoretyczne i symulację numeryczną charakterystyk dynamicznych systemu wrzeciona ze sprzężonym podwójnym rotorem w wiertarce dużej szybkości, Przeanalizowano i obliczono szybkości krytyczne trzech pierwszych rzędów, typy wibracji i inne parametry charakterystyk dynamicznych systemu wrzeciona. Wykazano, że szybkości krytyczne systemu z rotorem podwójnym odpowiadają szybkości krytycznej odpowiednika z rotorem pojedynczym. Natomiast typy wibracji każdego rzędu rotora podwójnego są superpozycją typów wibracji pojedynczych rotorów. Jeśli szybkość krytyczna systemu z podwójnym rotorem jest bliska tej, jaką ma pojedynczy rotor, typy wibracji pojedynczych rotorów stają się bardziej znaczące pod wpływem stanu sprzężenia.* ***Modelowanie i symulacja dynamiki systemu wrzeciona ze sprzężonym podwójnym rotorem w wiertarce dużych prędkości***

Keywords: High speed grinder, Coupled double-rotor spindle system, Dynamics modeling, Critical speeds.
Słowa kluczowe: Wiertarka dużych szybkości, System wrzeciona ze sprzężonym podwójnym rotorem, Modelowanie dynamiki, Szybkości krytyczne

Introduction

The spindle of high speed grinder is a typical high speed bearings-rotor dynamics system which is coupled double-rotor spindle system, and its rotating speed far surpasses the critical speed of the low order system. The realization of dynamic balance is associated with the performance and stability of the whole equipment [1-3]. The research of rotor dynamic balance mainly involved the rigid rotor before the 1950s. With the increase of the rotating speed and the flexibility of, the research on the method of flexible rotor's dynamic balance appeared. The early stage method of flexible rotor's dynamic balance was put forward by Federn, which was later called vibration balance method or modal balance method. The number of times of start-up of high-speed balance was relatively less, and is of high sensitivity [4-6]. The low order mode would not be affected when the balancing of high order mode was conducted, but identification was not balanced. The influence of bearing characteristics was especially great under large damping. It was not easy to achieve single mode when used near critical speed in shafting balance. Later the American Goodman formally presented influence coefficient method based on least square method, and its advantages were as follows: electronic computer could be used to assist dynamic balance; the identification of unbalance factors was not affected by bearing characteristics; it could balance several vibration models simutaneously, which was more convenient especially for the balance of the shafts. However, the number of times of start-up in high speed balance was more, and the susceptibility of high order modes was reduced. Based on the basic theories of rotor dynamics and structural system dynamics, dynamics theory model of the spindle system of high speed grinder was established using the transfer matrix method and the overall transfer matrix method in this study, and the simulation study was conducted on the influence of critical speed, vibration mode on the dynamic characteristics of coupled double-rotor spindle system of high speed grinder [7-9].

The dynamics modeling

High speed spindle system is a continuous elastomer. Based on the concentration mass dynamic modeling theory of the transfer matrix method, it was necessary to simplify the quality-continuous actual rotor into the rotor with a series of concentrated mass and rigid disks, which were connected by massless and flexible shaft sections in between. Threads and chamfers, as well as the influence of local non-circular section were ignored during the simplifying process of the spindle system before dispersing. High speed grinding spindle system mainly consisted of bearings, spindle, motor rotor, and additional parts (locking nut, bearing retainer ring, encoder, sealing rings, etc.). The structural diagram is shown in Figure 1.

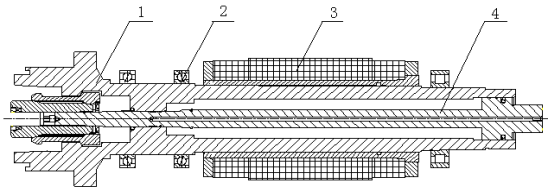

1-Rotor 1 2-Bearing 3-Motor rotor 4-Rotor 2
Fig.1 The structural diagram of spindle system

The bearing spindle system was generally divided into sliding bearing and rolling bearing. For sliding bearing, the oil film's dynamic coefficient matrix was as follows:

$$[C]=\begin{bmatrix} c_{xx} & c_{xy} \\ c_{yx} & c_{yy} \end{bmatrix};[K]=\begin{bmatrix} k_{xx} & k_{xy} \\ k_{yx} & k_{yy} \end{bmatrix} \tag{1}$$

The coefficient matrix of the dynamic performance of bearing block was as follows:

$$[C_b]=\begin{bmatrix} c_{bxx} & c_{bxy} \\ c_{byx} & c_{byy} \end{bmatrix};[K_b]=\begin{bmatrix} k_{bxx} & k_{bxy} \\ k_{byx} & k_{byy} \end{bmatrix} \tag{2}$$

When there was not too much difference in the stiffness and the equivalent mass of the bearing block in the direction of x, y, and coupling was relatively weak, the damping effect was negligible and the bearing was considered as isotropic:

(3)
$$k_{xx}=k_{yy};k_{bxx}=k_{byy};M_{bx}=M_{by}$$
$$k_{xy}=k_{yx}=k_{bxy}=k_{byx}=0$$

The model was converted to a fixed in-plane, and the rigidity coefficient of elastic bearing K could be calculated according to the formula below:

(4)
$$K=\frac{k_p(k_b-M_b\omega^2)}{k_p+k_b-M_b\omega^2}$$

K was the total bearing rigidity coefficient of the sliding bearing, which reflected the dynamic characteristics of the oil film, the bearing block and the foundation in a comprehensive way. The total bearing rigidity coefficient of the bearing was not constant, which was different from that of the common elastic bearing of equivalent stiffness, which was related to the whirling angular velocity of the rotor.

For rolling bearing, the radial stiffness of the two bearings could form a larger angular stiffness, which was calculated according to the formula below:

(5)
$$K_\theta=K_r(\frac{l^2}{4})$$

Where was the radial stiffness, was the center distance between series bearings. At this time, the bearing point was selected as of the midpoint of the line connected the centers of series bearings. When the mass of the bearing itself was taken into account, it could be treated as a concentrated mass point.

The spindle system was divided into several typical components or parts, such as concentrated mass, disc, shaft section and bearing. The two ends of the i unit was labeled with i and i+1, respectively, and the concentrated mass, disk and bearing etc. were focused on i point. Q_i,M_i,θ_i, X_i represented shear, bending, angle, deflection of the left end of i unit, respectively. Likewise, Q_{i+1},M_{i+1},θ_{i+1}, X_{i+1} represented shear, bending, angle, deflection of the right end of the i unit, respectively. The state vector could be expressed as $[Z]_i=[Q \quad M \quad \theta \quad X]_i^T$, and the relation between the state vectors of any two ends is shown below:

(6)
$$[Z]_{i+1}=[U]_i[Z]_i$$

where $[u]_i$ was a transfer matrix, which satisfied mechanic equilibrium and connected the state vectors of the two two sections of i and i+1.

Figure 2 shows a typical transfer matrix unit which consisted of a massless shaft of uniform section, a disk and an elastic bearing.

Then holistic transfer matrix is shown below:

$$\begin{bmatrix}Q\\M_1\\\theta_1\\X_1\\Q\\M_2\\\theta_2\\X_2\end{bmatrix}_{i+1}=\begin{bmatrix}1&0&0&m\Omega^2-K_y&0&0&0&0\\0&1&(J_p\frac{\omega}{\Omega}-J_d)\Omega^2+K_\theta&(m\Omega^2-K_y)l&0&0&0&0\\\frac{l^2}{2EI}&\frac{l}{EI}&1+\frac{l}{EI}[(J_p\frac{\omega}{\Omega}-J_d)\Omega^2+K_\theta]&\frac{l^2}{2EI}(m\Omega^2-K_y)&0&0&0&0\\\frac{l^3}{6EI}(1-\nu)&\frac{l^2}{2EI}&1+\frac{l^2}{2EI}[(J_p\frac{\omega}{\Omega}-J_d)\Omega^2+K_\theta]&1+\frac{l^3}{6EI}(1-\nu)(m\Omega^2-K_y)&0&0&0&0\\0&0&0&0&1&0&0&m\Omega^2-K_y\\0&0&0&0&l&1&(J_p\frac{\omega}{\Omega}-J_d)\Omega^2+K_\theta&(m\Omega^2-K_y)l\\0&0&0&0&\frac{l^2}{2EI}&\frac{l}{EI}&1+\frac{l}{EI}[(J_p\frac{\omega}{\Omega}-J_d)\Omega^2+K_\theta]&\frac{l^2}{2EI}(m\Omega^2-K_y)\\0&0&0&0&\frac{l^3}{6EI}(1-\nu)&\frac{l^2}{2EI}&1+\frac{l^2}{2EI}[(J_p\frac{\omega}{\Omega}-J_d)\Omega^2+K_\theta]&1+\frac{l^3}{6EI}(1-\nu)(m\Omega^2-K_y)\end{bmatrix}\begin{bmatrix}Q\\M_1\\\theta_1\\X_1\\Q\\M_2\\\theta_2\\X_2\end{bmatrix}_i$$

where l was the length of unit shaft; m was the total mass of the nodes (except the mass of shaft section, the roulette mass should be added.); Ω was angular velocity of precession of the rotor; ω was angular velocity of rotation of the rotor; J_d was the diameter moment of inertia of the rotor; J_p was the polar moment of inertia of the rotor; EI was the bending rigidity of the cross section of the shaft; G was the shear elastic modulus; A was the area of the cross section of the shaft; k_t was the coefficient of the shape of cross section, which was chosen as 2/3 when it was hollow circular cross section, and 0.9 when it was a solid one. Then coupled double-rotor transfer matrix is shown below:

(8)
$$\begin{bmatrix}Q^I\\M^I\\\theta^I\\X^I\\Q^{II}\\M^{II}\\\theta^{II}\\X^{II}\end{bmatrix}^R_i=\begin{bmatrix}1&0&0&-K_c&0&0&0&K_c\\0&1&K_{ch}&0&0&0&-K_{ch}&0\\0&0&1&0&0&0&0&0\\0&0&0&1&0&0&0&0\\0&0&0&K_c&1&0&0&-K_c\\0&0&-K_{ch}&0&0&1&K_{ch}&0\\0&0&0&0&0&0&1&0\\0&0&0&0&0&0&0&1\end{bmatrix}_i\begin{bmatrix}Q^I\\M^I\\\theta^I\\X^I\\Q^{II}\\M^{II}\\\theta^{II}\\X^{II}\end{bmatrix}^L_i$$

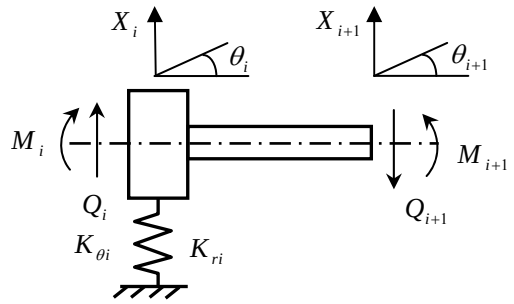

Fig.2 The typical transfer matrix unit

Mathematical model of critical speed and vibration mode

The state vector of section of the spindle terminal was as follows:

(9)
$$[Z]_{n+1}=[U]_n[U]_{n-1}\cdots[U]_{i+1}[RS][U]_i[U]_{i-1}\cdots[U]_1[Z]_0=[T][V]_1$$

Where [T] was 8×8 order matrix. The critical rotational speed during the synchronized process when Ω=ω was usually calculated. Therefore, the element in matrix [U] was the function of Ω. The boundary conditions that both sides were free ends were substituted, then:

(10)
$$[Z]_n=\begin{bmatrix}0\\0\\\theta\\X\end{bmatrix}_n=\begin{bmatrix}U_{11}&U_{12}&U_{13}&U_{14}\\U_{21}&U_{22}&U_{23}&U_{24}\\U_{31}&U_{32}&U_{33}&U_{34}\\U_{41}&U_{42}&U_{43}&U_{44}\end{bmatrix}\begin{bmatrix}0\\0\\\theta\\X\end{bmatrix}_0$$

The following result could be obtained:

(11)
$$\begin{bmatrix}U_{13}&U_{14}\\U_{23}&U_{24}\end{bmatrix}\begin{bmatrix}\theta\\X\end{bmatrix}_0=0$$

For the homogeneous equation to have non-trivial solutions, the following requirement must be satisfied:

(12)
$$f(\Omega)=\begin{vmatrix}U_{13}&U_{14}\\U_{23}&U_{24}\end{vmatrix}=0$$

f(Ω) was residual formula, and the solutions of equation f(Ω)=0 were the desired critical rotational speeds. The rope root law was applied to seek solutions in this paper.

The corresponding vibration mode could be calculated after the critical rotational speeds were obtained. A proportion solution could be obtained according to the homogeneous linear equation. For example, if θ_0=1, then X_0 could be calculated, and the initial state vector was thus obtained. According to Formula (9), the state vector of each computing website could be obtained. As a result, all the vibration modes in every order were known.

Critical speeds and mode of vibration

The main parameters of spindle system of HSG280 type are shown in Table 1. Precision angle contact ceramic ball bearings of HCB71909-E-T-P4S type and HCB71908-E-T-P4S type, which were manufactured by Germany FAG Company, were used as the front bearing and back bearing of spindle, respectively. The overall structure was back-to-back, and spring constant pressure preloading method was adopted.

Table1 Main parameters of HSG280 type spindle system

Rated Speed (r/min)	10000
Maximum Speed (r/min)	15000
Rated Torque (N·m)	51
Rated Power (kW)	31.5
Tool Interface	ER32
Lubrication Method	Grease Lubrication
Cooling Method	Water-cooling

Critical speed and vibration mode of rotor 1

We calculated the critical speeds of the first four orders of rotor 1 to be 64440r/min 、 68940r/min 、 169980r/min 、 299940r/min, considering shear and gyroscopic effect; the corresponding main vibration modes of each order are shown in the Fig.2.

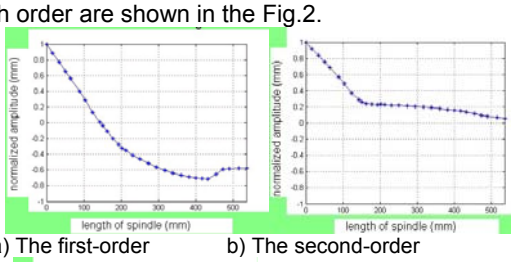

a) The first-order b) The second-order

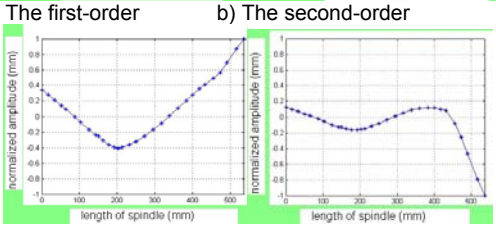

c) The third-order d) The fourth-order

Fig.2 The main vibration modes of the first four orders of rotor 1

It can be seen from the Fig.2 that for first-order main vibration mode, deformation of the spindle's front and back ends as well as the back bearing was larger, but that of the front bearing was smaller. The main vibration mode was swing vibration mode of front and back ends of spindle about the front bearing. The major reason for this phenomenon was that the rigidity of the front bearing, compared with that of the back bearing, was greater by one order of magnitude, with higher angular rigidity. In comparison, the rigidity of back bearing was lower. The second-order main vibration mode was swing vibration mode of front overhang. Third-order main vibration mode was first-order bending mode of the spindle, with the greatest vibration amplitude at back end of the spindle. Again, the back bearing had insufficient rigidity. Fourth-order main vibration mode was second-order bending mode of the spindle.

Critical speed and vibration mode of rotor 2

When calculating the critical speeds of rotor 2, we considered the coupling position as the bearing position. Thus, the critical speeds of the first four orders were calculated to be17820r/min、41880 r/min、116100 r/min、222240 r/min. The corresponding vibration mode is shown in the Fig.3.

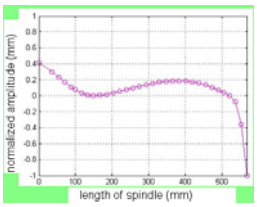

a) The first-order

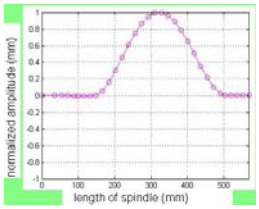

b) The second-order

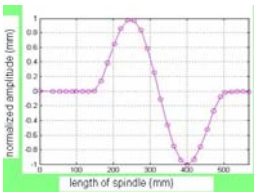

c) The third-order

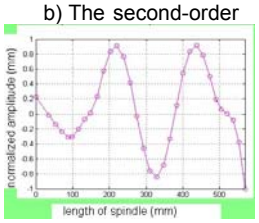

d) The fourth-order

Fig.3 The main vibration modes of the first four orders of rotor 2

It can be seen from the Fig.3 that the first-order main vibration mode of rotor 2 was swing vibration of front and back overhangs. Its second-order main vibration mode was first-order bending of the middle of rotor; the third-order main vibration mode was second-order bending of the rotor. The fourth-order vibration modes were quite complicated, including the third-order bending of the middle of rotor, first-order bending of the front overhang and swing vibration of the back overhang.

Critical speed and vibration mode of coupled double rotors

We calculated the critical speeds of the first six orders of coupled double rotors under the coupling between rotor 1 and 2 (as shown in the Fig.4).

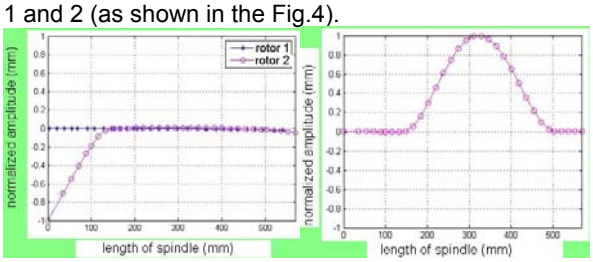

a) The first-order b) The second-order

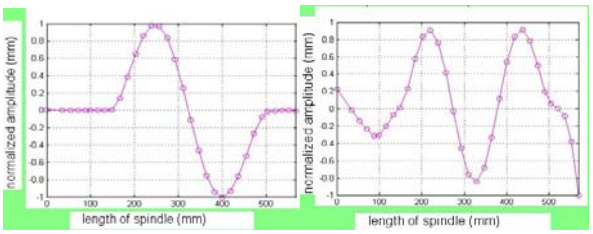

c) The fifth –order d) The sixth-order

Fig.4 The main vibration modes of the first six orders of coupled double-rotor

From the Fig.4 we can see that first-order and second-order vibration modes were respectively swing vibration of the front end of rotor 2 and first-order bending of the middle of rotor; third-order and fourth-order main vibration modes were swing vibration of rotor 1, accompanied by swing vibration of rotor 2. Fifth-order main vibration mode was second-order bending of the middle of rotor 2; sixth-order main vibration modes included first-order bending of rotor 1 and third-order bending of rotor 2. The data indicated that vibration mode of each order of double rotors

was the superimposition of the vibration mode of each single rotor. At variable critical speeds, the vibration mode of each single rotor in the system varied in its extent. If the critical speed of double-rotor system was close to that of a single rotor, then the superimposition of vibration modes of single rotors would become more significant under coupling state.

Conclusions

(1) The numerical results of modes of vibration of the first six orders reveals that the primary mode of vibration has the rotholes at the front end and the middle part of the spindle, the second-order mode of vibration mainly at the front end of the spindle, and the third-order mode of vibration mainly at the rear end. (2) the critical speeds of each order for coupled double-rotor system were lower than those of single rotor. This was especially the case at higher orders, which indicated that the coupling between rotors reduced critical speed of the entire system. The first-order and second-order critical speeds of double rotors were close to those of rotor 2; the third-order and fourth-order critical speeds of double rotors were close to the first-order and second-order critical speeds of rotor 1. Fifth-order critical speed of double rotors was close to third-order critical speed of rotor 2; sixth-order critical speed of double rotors was close to third-order critical speed of rotor 1. At higher orders, the critical speeds of two single rotors arranged in an increasing order corresponded to those of double rotors arranged in an increasing order. This implied that the critical speeds of double rotors were closely related to those of single rotor.

Acknowledgments

This research was financially supported by the National Natural Science Foundation of China (50875138; 51175276); the Shandong Provincial Natural Science Foundation of China (ZR2009FZ007);Qingdao science and technology program of basic research projects（12-1-4-4-(1)-jch）and the Specialized Construct Fund for Taishan Scholars.

REFERENCES

[1] Li C.H, Hou Y.L, Liu Z.R, Ding Y.C. Investigation into temperature field of nano-zirconia ceramics precision grinding, International Journal of Abrasive Technology, 4 (2011), No.1, 77 - 89

[2] Li Changhe, Hou Yali Chao Du and Ding Yucheng. An Analysis of the Electric Spindle's Dynamic Characteristics of High Speed Grinder, Journal of Advanced Manufacturing Systems, 10 (2011), No.1, 159–166

[3] Moulik P.N., Yang H.T.Y., Chandrasekar S. Simulation of thermal stresses due to grinding, International Journal of Mechanical Sciences, 43 (2001), No.3, 831-851

[4] Xiu S.C, Chao C.X. and Pei S.Y. Experimental research on surface integrity with less or non fluid grinding process, Key Engineering Materials, 487(2011), 89-93

[5] Zhu Lida, Wang Wanshan. Modeling and Experiment of Dynamic Performance of the Linear Rolling Guide in Turn-milling Centre, Advanced Science Letter, 4, (2011), No.6, 1913–1917

[6] Li Changhe, Hou Yali, J Li ingyao, et al. Mathematical modeling and simulation of fluid velocity field in grinding zone with smooth grinding wheel, Advanced Science Letter, 4(2011),No.6-7, 2468-2473

[7] Hou Yali, Li Changhe, Han Zhenlu et al. Examination of the Material Removal Mechanisms During the Abrasive Jet Finishing of 45 Steel. Advanced Science Letter, 4 (2011), No.4-5,1478-1484

[8] Li C.H, Hou Y. L, Fang Z, et al. Analytical and Experimental Investigation of Grinding Fluid Hydrodynamic Pressure at Wedge-shaped Zone. International Journal of Abrasive Technology, 4 (2011), No.2, 140 - 155

[9] Li Changhe, Hou Yali, Ding Yucheng,et al. Feasibility investigations on compound process: a novel fabrication method for finishing with grinding wheel as restraint. International Journal of Computational Materials Science and Surface Engineering, 4 (2011), No.1, 55 – 68

***Authors**: Engineer, Hou Yali, School of Mechanical Engineering, Qingdao Technological University, E-mail:houyalichina@163.com; Wang Sheng, E-mail: wangsheng8802@163.com; Han Zhenlu, E-mail: hanzhenlux@163.com.*